PHYSICAL REVIEW D VOLUME 17, NUMBER 4 15 FEBRUARY 1978

Rutherford scattering with radiation reaction

J. Huschilt and W. E. Baylis
Department of Physics, University of Windsor, Windsor, Ontario, Canada N9B 3P4
(Received 4 November 1977)

Numerical solutions of the Lorentz-Dirac equation are presented for the scattering of a spinless point particle in the static Coulomb field of a fixed point of opposite charge. Within the framework of classical electrodynamics, radiation reaction has thus been included exactly. For any initial energy, there is a minimum impact parameter below which the particle is captured. The classical capture cross section is readily found and is presented here as a function of incident energy. Scattering cross sections for a fixed initial energy ($\simeq 10^3 mc^2$) are also presented and compared with those for relativistic Rutherford scattering. Loss of energy and angular momentum to radiation is calculated, and the total energy (particle plus radiation) is found to be accurately conserved in all cases not involving capture. Radiation reaction is seen frequently to cause the projectile to accelerate *away* from the *attractive* scattering center.

I. INTRODUCTION

The pursuit of a satisfactory equation of motion which describes the trajectories of charged particles in classical electrodynamics when the effect of radiation is included, and which may provide basic insight into related problems in quantum electrodynamics, is one of continuing importance and interest.[1-5] Such an equation can be tested by seeing how its solutions behave for the simplest problems, those involving two particles colliding along a line or in a plane, interacting through their own fields. In this way, we have been able to show that some of the proposed equations which reduce to the Lorentz equation for two like charges moving directly toward each other give apparently unphysical results.[6-8] In other recent papers,[9,10] we have presented numerical solutions to the problem of two charges, like and unlike, colliding head-on under their retarded fields, with radiation-reaction effects included as prescribed by the Lorentz-Dirac equation.[11,12] For like charges (repulsive case) thrown together from large distances even at highly relativistic speeds (up to $v_I = 0.99c$), trajectories which are physically reasonable are obtained. The colliding particles always lose a small fraction of their kinetic energy during the collision to radiation, and compared with computations without radiation, the maximum accelerations are smaller and the distances of closest approach larger. In particular, when one of the particles is infinitely massive, the other particle loses an amount of kinetic energy equal to the energy radiated during collision. However, when unlike charges (attractive case) are released from rest, both of like mass or one of infinite mass (say with a positive charge), we find that no physical solutions exist with finite initial values of position, energy, and acceleration. This result may be ascribed to the nonlocality of the Lorentz-Dirac equation[13] and the infinite field strength of a point particle at its position.

It is of considerable interest to see what happens for scattering with a *finite* initial impact parameter b_I from a fixed point charge, and to study the results as the ratio of b_I to the classical electron radius approaches zero. In this paper then, we present numerical solutions of the Lorentz-Dirac equation for the scattering of a spinless point particle in the static Coulomb field of a fixed point of opposite charge. In Sec. II, we first present the two-dimensional, third-order differential equations which must be solved, along with a brief description of the numerical approach. In Sec. III, we present the results at capture threshold, i.e., trajectories for which the final particle energy is its rest-mass energy. Comparisons of calculated trajectories both with and without radiation reaction are given. Then (Sec. IV) we present scattering cross sections for initial kinetic energies of 550 MeV and compare them with results of relativistic Rutherford scattering, in which radiation reaction is neglected. Next (Sec. V) we mention some unusual trajectory behavior especially for small impact parameter b_I, wherein the projectile early in its trajectory is seen to have an acceleration component directed *away* from the attractive center even at very large separations. Conclusions and a brief discussion of the significance of these results follow (Sec. VI). We have investigated solutions of the Lorentz-Dirac equation with emphasis on their behavior in the limits of large and small impact parameter.

II. THE PROBLEM AND NUMERICAL METHOD

Numerical investigations of the scattering of two unlike charges of equal mass with nonzero impact parameter are formidable. Both acceleration and velocity parts of retarded magnetic and retarded electric fields must be considered. When the Lorentz-Dirac equation is used to include the ef-

fects of radiation, the additional problem of selecting out a physical solution by imposing the usual condition that the acceleration $|\vec{a}| \to 0$ as $t \to +\infty$ seems to make the problem even more intractable. Fortunately, as we have seen in the head-on collisions of like charges, essential features of the collision can be obtained when one of the particles is infinitely massive so that the light particle moves in the static field of the other.[9] The boundary condition is easily met by integrating backwards in time, and besides, confidence in the numerical solution can be obtained by comparing the kinetic energy lost by the incident particle with the computed (Larmor) energy radiated during the collision.

Thus, we consider here collisions of two unlike charges: one of finite mass, an electron say, and the other a very massive "proton," where there is a finite impact parameter. In Sec. III, our "starting" conditions guarantee that the incident particle just escapes to infinity so that capture cross sections may be calculated. In Sec. IV, the starting conditions are chosen so as to effectively vary the impact parameter b_I for a constant initial-particle kinetic energy of 550 MeV ($\approx 10^3 mc^2$).

The Lorentz-Dirac equation for a particle of charge e and rest mass m is

$$ma^\mu = eF^{\mu\nu}u_\nu + \tfrac{2}{3}e^2(da^\mu/d\tau + a^\nu a_\nu u^\mu), \tag{1}$$

where $F^{\mu\nu}$ is the external (static) field of the massive particle and τ, $u^\mu \equiv dx^\mu/d\tau$, and $a^\mu \equiv du^\mu/d\tau$ are the proper time, the four-velocity, and the four-acceleration, respectively (and $c=1$). Taking the x-y plane to be the plane of the collision (and with $e=m=1$, so that the unit of distance is $r_0 = e^2/mc^2$, the classical electron radius, and the unit of time is r_0/c) the equation of motion becomes

$$\ddot{x} = -\tfrac{3}{2}\gamma^{-4}E_x(1+\gamma^2\dot{y}^2) + \tfrac{3}{2}\gamma^{-2}E_y\dot{x}\dot{y} - 3\gamma^2(\dot{x}\ddot{x}+\dot{y}\ddot{y})\dot{x} + \tfrac{3}{2}\gamma^{-1}\ddot{x}, \tag{2a}$$

$$\ddot{y} = -\tfrac{3}{2}\gamma^{-4}E_y(1+\gamma^2\dot{x}^2) + \tfrac{3}{2}\gamma^{-2}E_x\dot{x}\dot{y} - 3\gamma^2(\dot{x}\ddot{x}+\dot{y}\ddot{y})\dot{y} + \tfrac{3}{2}\gamma^{-1}\ddot{y}, \tag{2b}$$

where the electric field components are

$$E_x = -\frac{x}{r^3}, \quad E_y = -\frac{y}{r^3},$$

with

$$r = (x^2+y^2)^{1/2},$$

$$\gamma = (1-v^2)^{-1/2},$$

$$v = (\dot{x}^2+\dot{y}^2)^{1/2},$$

and dots over a variable indicate differentiation with respect to ordinary time t. The equations are obviously a set of two simultaneous ordinary differential equations of third order.

The calculations were made in double precision on an IBM 360-65 computer using a Hamming predictor-corrector integration method essentially as previously described and found reliable.[9,10] The "starting" conditions were typically (at $t=0$)

$$x_f = 1000, \quad y_f = b_f \text{ (variable)},$$

$$\dot{x}_f = v_f, \quad \dot{y}_f = 0,$$

$$\ddot{x}_f = (\gamma^{-3}E_x)_f, \quad \ddot{y}_f = (\gamma^{-1}E_y)_f.$$

The v_f was adjusted to achieve the objectives treated in Secs. III and IV. The given $\ddot{x}_f$ and $\ddot{y}_f$ are the Lorentz (no radiation reaction) values. The integration was carried backwards in time to $t=t_i$ sufficiently early so that preacceleration effects were then negligible (see Sec. V). To obtain the total scattering angle, both ends ($t=t_f=0$ to $t=+\infty$ and $t=-\infty$ to $t=t_i$) were fitted to Lorentz scattering. The corrected (initial) impact parameter $b_I(t=-\infty)$ is obtained from $b_i(t=t_i)$ by assuming constant angular momentum and constant total particle energy between these times. See also the Appendix for a treatment of relativistic inverse-square orbits and a derivation of the relativistic Rutherford scattering formula.

The test of energy conservation, which served as a check on the computational reliability, was as follows. Letting $\mu=0$ in Eq. (1), we obtain

$$a^0 = F^{0\nu}u_\nu + \tfrac{2}{3}\left(\frac{da^0}{d\tau} + a^2u^0\right), \tag{3}$$

where $a^2 = a^\nu a_\nu = (a^0)^2 - (\vec{a})^2$, $F^{0\nu}u_\nu = \gamma\vec{E}\cdot\vec{v}$, $a^0 = d\gamma/d\tau = \gamma^4\vec{a}\cdot\vec{v}$. Integrating with respect to τ between τ_1 and τ_2, and using $\gamma d\tau = dt$, we obtain

$$\Delta\gamma\big|_1^2 = \int_1^2 \vec{E}\cdot\vec{v}\,dt + \tfrac{2}{3}\int_1^2 da^0 + \tfrac{2}{3}\int_1^2 a^2 dt. \tag{4}$$

Now the Larmor power[14] is just $P = -\frac{2}{3}a^2$, and $\int_1^2 \vec{E}\cdot\vec{v}\,dt = \int_1^2 \vec{E}\cdot d\vec{x} = \Phi(1) - \Phi(2)$, where $\Phi(r)$ is the electrostatic potential energy. Letting the limits 2 and 1 correspond to $t_2 = +\infty$ and $t_i = t < 0$, respectively, we have, after rearranging terms slightly,

$$\gamma(t) - \gamma(\infty) = E_{\text{rad}} + \tfrac{2}{3}(\gamma^4\vec{a}\cdot\vec{v})_t - \Phi(r), \tag{5}$$

where we have used $\Phi(\infty) = 0 = \frac{2}{3}(\gamma^4\vec{a}\cdot\vec{v})_\infty$. $E_{\text{rad}} \equiv \int_t^\infty P\,dt$ represents the energy radiated from $t(<0)$ to $t=\infty$, but in practice the upper limit is taken to be $t=t_f=0$, assuming justifiably that the energy radiated between $t=0$ and $t=\infty$ is negligible. The term $\frac{2}{3}\gamma^4(\vec{a}\cdot\vec{v})_t$ is, of course, the Schott energy. Computed values of the left-hand side, the particle energy lost, invariably agreed well with those of the right-hand side whenever calculated. At times

$t=t_i$ where the Schott energy and the potential energy are negligible, the (kinetic) energy lost equals the energy radiated by the particle during the collision.

III. CAPTURE CROSS SECTION

Among the peculiar properties of the Lorentz-Dirac equation is that it does not admit a physical solution for capture of a point particle by a fixed charge in a head-on collision.[10] Solutions of the Lorentz-Dirac equation involving capture with two-dimensional motion obviously cannot be treated as described above (Sec. II) and are not considered here. Instead we investigate threshold solutions for which the final velocity is zero, i.e., $\gamma_F = \gamma(t=+\infty)=1$.

The starting value of $\dot{x}_f = v_f(t=t_f=0)$ required at capture threshold, assuming there is no radiation loss after $t=0$, is easily determined to be $v_f = (1-\gamma_f^{-2})^{1/2}$, where $\gamma_f = 1+1/r_f$, $r_f=(x_f^2+y_f^2)^{1/2}$. For a value of $x_f=1000$, $y_f=b_f$ was varied from 100 to 5. As a result, the impact parameter b_I, corresponding to $t=-\infty$, varied from 49.2 to 0.190, the distance of closest approach, $r_{\min}$, ranged from 9.78 to 0.134, and the capture scattering cross section $\sigma_{cap}\equiv\pi b_I^2$ ranged from 7.62×10^3 to 0.114. At the same time, loss in particle energy ranged over almost nine orders of magnitude from 4.6×10^{-3} to 1.8×10^6, respectively. A plot of b_I, $r_{\min}$, and $\sigma=\sigma_{cap}$ vs $-\Delta\gamma\equiv\gamma_I-1$, the loss in particle energy (or energy radiated), is given in Fig. 1. For $b_I\simeq1.0$, $r_{\min}\simeq0.55$, the energy radiated is

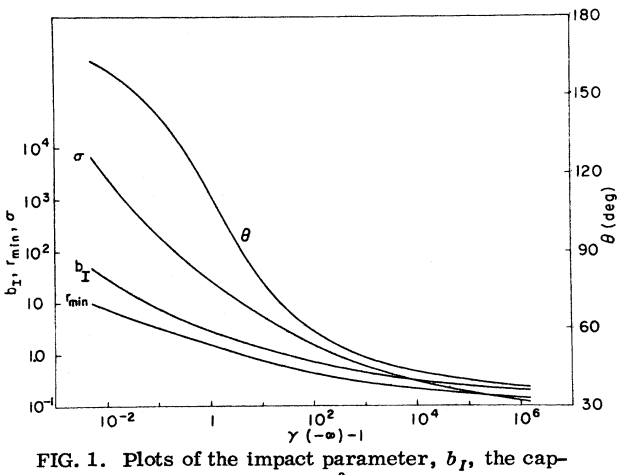

FIG. 1. Plots of the impact parameter, b_I, the capture cross section, $\sigma\equiv\sigma_{cap}=\pi b_I^2$, the distance of closest approach, $r_{\min}$, and the maximum scattering angle, θ (i.e. the scattering angle at threshold) against the loss in particle energy (or, equivalently, energy radiated during the collision), $-\Delta\gamma=\gamma(-\infty)-1$, at capture threshold.

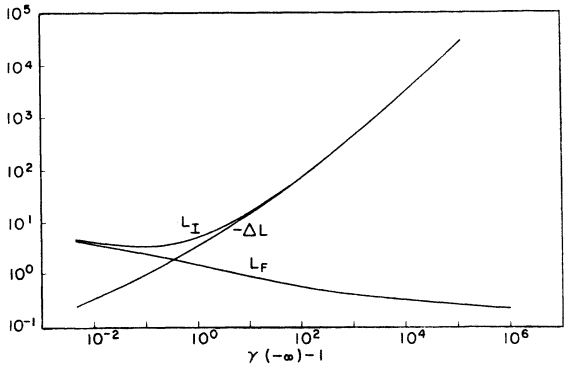

FIG. 2. Graphs of the initial angular momentum, L_I, the final angular momentum, L_F, and the loss in angular momentum, $-\Delta L\equiv L_I-L_F$, as a function of the loss in particle energy (or the energy radiated or the initial-particle kinetic energy), $-\Delta\gamma\equiv\gamma(-\infty)-1$, at capture threshold. There is a minimun in L_I of about 3.5 for $-\Delta\gamma\simeq0.11$, at which $b_I\simeq7.3$ and $r_{\min}\simeq3.2$. (Incidentally, according to quantum mechanics, the smallest value of the orbital angular momentum is $L=\hbar$, which in our units is the reciprocal of the fine-structure constant, i.e., ≃137.)

≃28, while for $b_I\simeq2.9$, $r_{\min}\simeq1.5$, the energy radiated is still ≃1.0 (one electron rest mass). In each case, the energy radiated by the particle during collision as computed by the relativistic Larmor power formula,[14]

$$P=-\tfrac{2}{3}a^2=\tfrac{2}{3}\gamma^6[\vec{a}^2-(\vec{v}\times\vec{a})^2]$$
$$=\tfrac{2}{3}\gamma^6[(\ddot{x}^2+\ddot{y}^2)-(\dot{x}\ddot{y}-\dot{y}\ddot{x})^2], \qquad (6)$$

was in excellent agreement with the kinetic energy lost by the particle. However, an interesting effect was that the computations had to be carried out to increasingly earlier times to obtain this agreement for the lower starting values of b_f corresponding to the smaller values of b_I. This phenomenon is discussed further in Sec. V. It is notable that when the impact parameter b_I is decreased below 1, the initial particle energy required for a physical solution at capture threshold increases dramatically, apparently without limit as $b_I\to0$.

For the range of parameter values used (see above), the threshold scattering angle, θ, ranges from 164.5° to 36.4°. Figure 1 also gives a plot of the loss in particle energy vs the scattering angle. As might be expected, the larger threshold scattering angles correspond to larger impact parameters and to smaller initial energy. Incidentally, for an initial kinetic energy of $\gamma_I-1=1076.32=550$ MeV, the threshold scattering angle is 48.82°.

Finally, again for the ranges stated above, the initial (orbital) angular momentum, L_I, ranges

from 4.71 to 3.43×10^5, the final angular momentum, L_F, ranges from 4.46 to 0.223, and the change $-\Delta L \equiv L_I - L_F$ ranges from 0.252 to 3.43×10^5. Figure 2 shows the dependence of L_I, L_F, and $-\Delta L$ on the loss in particle energy. There is a minimum in L_I of $\simeq 3.5$ for $-\Delta\gamma \simeq 0.11$ at which $b_I \simeq 7.3$ and $r_{\min} \simeq 3.2$. Both L_I and $-\Delta L$ appear to increase without bounds as b_I decreases to zero. Quantum mechanically, the smallest value of the (orbital) angular momentum is $L = \hbar$, which in our units is the reciprocal of the fine-structure constant ($\alpha = e^2/c\hbar$), i.e., $\simeq 137.04$. The Compton wavelength for an electron is $\hbar/m_0 c$ which has the same numerical value.

Our computer calculations indicate that at capture threshold, as b_I is increased steadily above ~1, the Lorentz-Dirac equation predicts physically reasonable solutions: Less and less energy is lost to radiation, the initial angular momentum increases (after a minimum of $\simeq 3.5$), the loss in angular momentum decreases towards zero, and the particle scatters through increasingly larger angles. In short, the behavior of the Lorentz-Dirac equation approaches that of the Lorentz equation in this limit, as is expected. However, when b_I is effectively decreased below ~1, the threshold scattering angle decreases, while the necessary incident energy and the energy radiated, as well as the initial angular momentum and its change, all increase dramatically, apparently without limit. These results are consistent with and approach those found for head-on collisions with $b_I = 0$, where there are no physical solutions for finite initial values.[10]

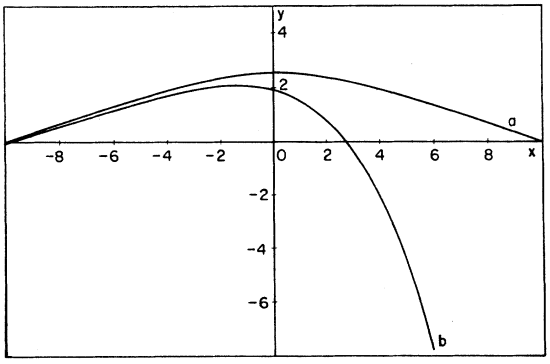

FIG. 3. Scattering curves for an incident-particle energy, angular momentum, and impact parameter of $\gamma_I = 1.558$, $L_I = 4.309$, $b_I = 3.604$, respectively; (a) without radiation reaction, for which $\gamma_F = \gamma_I$, $L_F = L_I$, $r_{\min} = 2.581$, and $\theta = 40.58°$ and (b) with radiation reaction, for which $\gamma_F = 1$, $L_F = 1.788$, $r_{\min} = 1.837$ (>1), and $\theta = 120.83°$. The y axis is chosen as the symmetry axis for curve a.

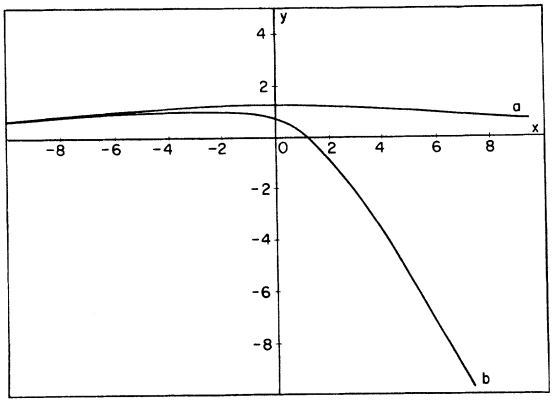

FIG. 4. Similar to Fig. 3, but $\gamma_I = 12.929$, $L_I = 16.844$, $b_I = 1.307$; (a) without radiation reaction for which $\gamma_F = \gamma_I$, $L_F = L_I$, $r_{\min} = 1.229$ and $\theta = 7.16°$, and (b) with radiation reaction, for which $\gamma_F = 1$, $L_F = 0.894$, $r_{\min} = 0.693$ (<1) and $\theta = 76.39°$.

The effects of radiation trajectories both without radiation reaction (curve a) and with (curve b) are shown in Figs. 3 and 4 for the typical case of $r_{\min} \gtrsim 1$ and $r_{\min} \lesssim 1$, respectively. The y axis is chosen as the axis of symmetry for curve a in each figure. The effects of radiation as predicted by the Lorentz-Dirac equation make physical sense. Compared with computations without radiation reaction, the distances of closest approach are smaller, the maximum accelerations and the scattering angles are larger.

IV. SCATTERING CROSS SECTIONS AT FIXED ENERGY

The scattering of a particle of fixed initial energy as a function of impact parameter b_I is now considered. We have chosen a value of $\gamma_I = 1077.32$, which is equivalent to an initial particle kinetic energy of $\gamma_I - 1 = 1076.32 = 550$ MeV for a particle with the rest mass of an electron. In this case, with a starting value of $x_f = 1000$ (at $t = 0$) and with $y_f = b_f$, an iterative procedure is used to vary $\dot{x}_f = v_f$ ($y_f = 0$) until the desired initial energy is obtained. At the lower values of b_I, the computations once again had to be extended to larger separations, but to a lesser extent than for high energies at threshold (Sec. III, see also Sec. V). We have computed results for which the impact parameter ranged from 60 down to a minimum of 0.4255 at capture threshold. The corresponding scattering angle was found to range from 1.78×10^{-3} degrees to a maximum of 48.82 degrees. Figure 5 shows the relation between b_I and θ, with an insert covering the range in θ from 25° to the maximum of 48.82°. A graph of $d\sigma/d\Omega = (b/\sin\theta)|db/d\theta|$ vs θ, obtained by numerical differentiation of $b_I(\theta)$, is

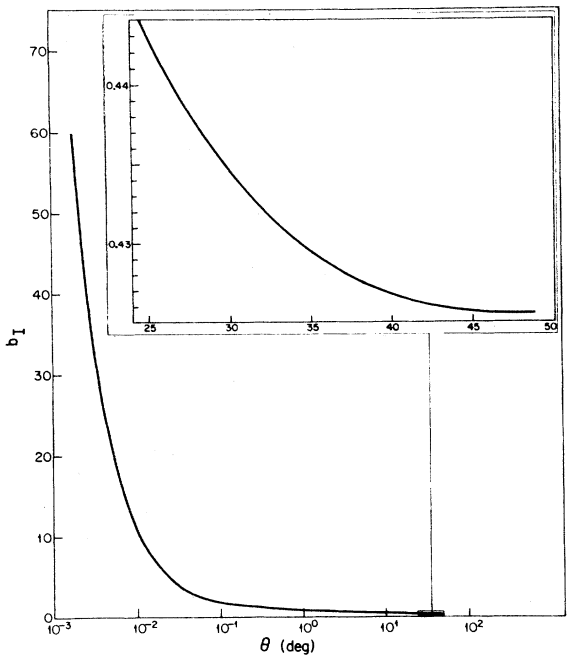

FIG. 5. The relation between the impact parameter, b_I, and the scattering angle, θ, for an initial-particle kinetic energy of $\gamma_I - 1 = 1076.32 = 550$ MeV. The insert gives an enlargement for the range in θ from $\simeq 25°$ to just beyond the maximum angle of 48.82°.

given in Fig. 6. For the range of angles plotted, $d\sigma/d\Omega$ varies over approximately nine orders of magnitude. For comparison, a graph of the relativistic Rutherford (see the Appendix for a derivation) differential scattering cross section is also given. The Lorentz-Dirac curve agrees with the Rutherford one within 10% only for very small angles $\theta \lesssim 0.01°$ where $d\sigma/d\Omega \gtrsim 2 \times 10^{-16}$ cm^2/sr.

The Lorentz-Dirac curve deviates from the Rutherford results by more than about three orders of magnitude for $\theta \gtrsim 40°$ where it drops sharply to the maximum scattering angle of 48.82° at capture threshold.

The relations between the particle energy lost or the energy radiated, the impact parameter, and the scattering angle are given in the next two figures. The same procedure as mentioned in the preceding section was followed to obtain the corrected impact parameter b_I and the total scattering angle. Over the range of b_I used ($0.42 \lesssim b_I \lesssim 60$), the loss in particle energy varies from 0.53 to 1076.32. Figure 7 is a graph of the particle energy lost, $-\Delta\gamma$, and the distance of closest approach, $r_{\min}$, vs the impact parameter. For the larger values of b_I, $r_{\min}$ approaches b_I consistent with the associated very small scattering angles. For $b_I \simeq 1.45$, $r_{\min} \simeq 1.00$ and the particle energy loss is $\simeq 790$, whereas for $b_I \simeq 1.00$, $r_{\min} \simeq 0.67$ and the particle energy loss is $\simeq 960$. At capture threshold, for which the impact parameter is 0.4255, the distance of closest approach is 0.2776. Figure 8 depicts the variation of the final particle energy, γ_F, with the scattering angle. About one rest mass is radiated away for as large an impact parameter as $b_I \simeq 44$, for which the scattering angle is only $\simeq 2.4 \times 10^{-3}$ degrees. Of course, all of the incident kinetic energy is radiated away when the scattering angle is 48.82°, corresponding to an impact parameter of 0.4255. As in the threshold calculations above, good agreement between the particle energy lost and the energy radiated during the collision was confirmed for all the runs in this case as well.

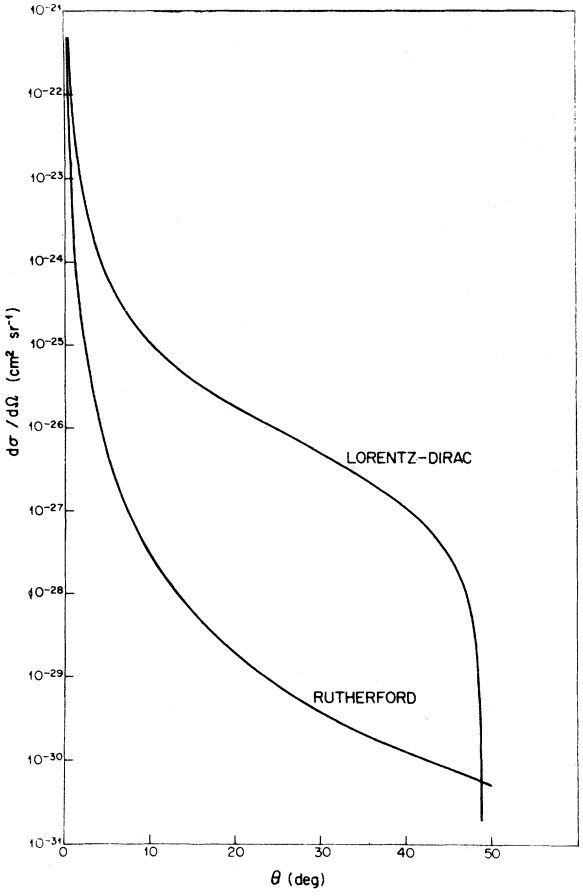

FIG. 6. Plots of the differential scattering cross section, $d\sigma/d\Omega$ for Lorentz-Dirac and relativistic Rutherford scattering vs the scattering angle, θ, for initial-particle kinetic energies of 550 MeV. The Lorentz-Dirac curve agrees with the Rutherford within 10% only for very small angles, $\theta \lesssim 0.01°$, where $d\sigma/d\Omega \gtrsim 2 \times 10^{-16}$. The curves deviate markedly from each other as θ increases until about $\theta \gtrsim 40°$, where it drops sharply at the maximum scattering angle of 48.82° at capture threshold.

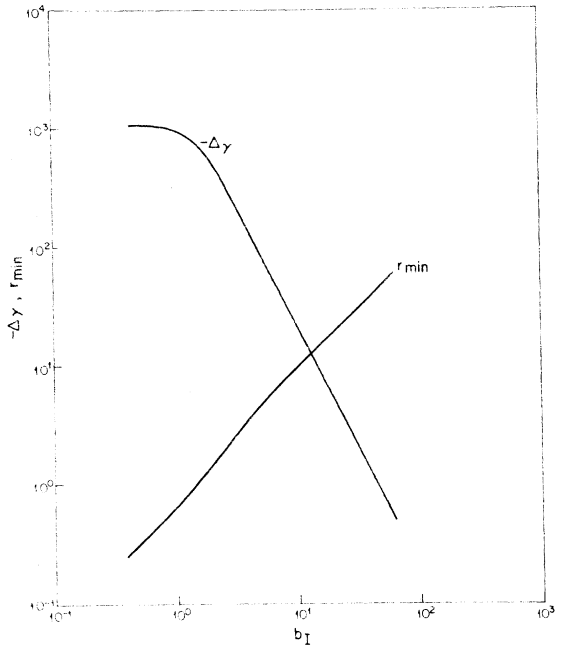

FIG. 7. The particle energy lost, $-\Delta\gamma$ (or the energy radiated during collision) and the distance of closest approach, r_{min}, as a function of the impact parameter, b_I, for initial particle kinetic energies of 550 MeV. For relatively large b_I, r_{min} is barely smaller than b_I corresponding to small scattering angles. For $b_I \simeq 1.45$, $r_{min} \simeq 1.00$ and $-\Delta\gamma \simeq 790$, while for $b_I \simeq 1.00$, $r_{min} \simeq 0.67$ and $-\Delta\gamma \simeq 960$. At capture threshold $b_I = 0.4255$ with $r_{min} = 0.2776$. See also Fig. 8.

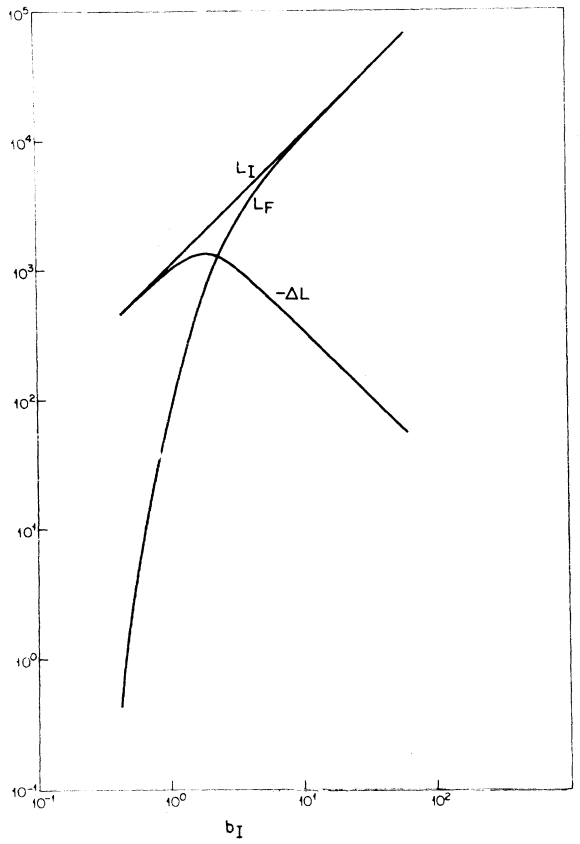

FIG. 9. Plots of L_I, L_F, and $-\Delta L \equiv L_I - L_F$, the initial, final, and loss in angular momentum, respectively, vs the impact parameter, b_I, for an initial particle kinetic energy of 550 MeV. There is a maximum loss in angular momentum of $-\Delta L \simeq 1.35 \times 10^3$ for $b_I \simeq 1.85$, for which $r_{min} \simeq 1.35$, $-\Delta L \simeq 620$, and $\theta \simeq 0.11°$.

For the ranges previously cited, the initial angular momentum, L_I, ranges from 6.47×10^4 to 458.4, the final angular momentum, L_F, ranges from 6.46×10^4 to 0.42, and the loss in angular momentum, $-\Delta L \equiv L_I - L_F$, ranges from 55.92 to 457.9. In Fig. 9 we display graphs of L_I, L_F, and $-\Delta L$ vs the impact parameter, b_I. There is a maximum in the loss, $-\Delta L$, of $\simeq 1.35 \times 10^3$ for which $b_I \simeq 1.85$, $r_{min} \simeq 1.35$, $-\Delta\gamma \simeq 620$, and $\theta \simeq 0.11°$.

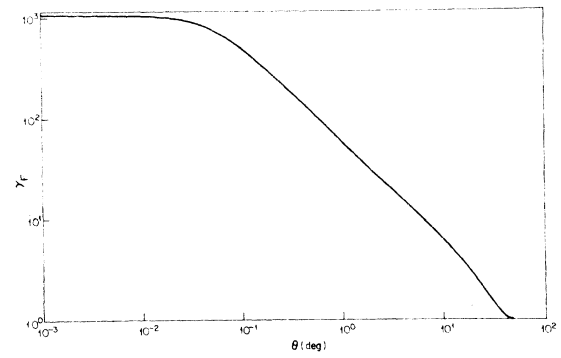

FIG. 8. The final-particle energy, γ_F, as a function of the scattering angle, θ, for an initial particle kinetic energy of $\gamma_I - 1 = 1076.32 = 550$ MeV. Approximately one rest mass is radiated away when $b_I \simeq 44$, for which $\theta \simeq 2.4 \times 10^{-3}$ deg. All of the incident kinetic energy is radiated away when $b_I = 0.4255$, for which $\theta = 48.82°$.

The property that the Lorentz-Dirac equation reverts to the Lorentz equation when the impact parameter increases recurs here for the case of constant initial energy of the incident particle. That the initial angular momentum should increase and its loss should decrease as b_I increases also makes physical sense. Physical solutions apparently exist right down to the capture threshold value of $b_I = 0.4255$, but rather large amounts of energy are lost due to radiation (for example, energy $\gtrsim 100$ rest masses is radiated for $b_I \lesssim 4.7$), and trajectories often display unexpected behavior.

V. UNEXPECTED TRAJECTORY BEHAVIOR

The first trajectories computed were those corresponding to the relatively large impact parameter $b_I \gtrsim 3$ ($b_f \gtrsim 35$) for the case of $\gamma_F = 1$. These trajectories behaved quite reasonably: Relatively little energy was radiated, the computations could be terminated when the scattered particle was as far away (at $t = t_i < 0$) as it was originally (at $t = t_f = 0$), namely approximately 1000 units. In addition, the sign of $\vec{a} \cdot \vec{v}$ (which was monitored throughout the collision, as well as its value) changed from positive to negative shortly before the collision indicating that the component of the acceleration, $\vec{a}$, was initially in the direction of the velocity until shortly before the collision. However, as the impact parameter was effectively decreased, it was noted that $\vec{a} \cdot \vec{v}$ changed sign at increasingly earlier times. Furthermore, agreement between the particle energy lost and the energy radiated could not be obtained until the integration was continued to include such times. Yet another peculiar behavior was noted in the ratio of $|\dot{\vec{p}}|$, the time rate of change of momentum ($\vec{p} = \gamma \vec{v}$), to the field $|\vec{E}|$. When there is no radiation reaction, the equation of motion is, of course, the Lorentz equation, which in our units is[15]

$$\dot{\vec{p}} = \vec{E} . \tag{7}$$

We can note the deviation from relativistic Rutherford scattering (as predicted by the Lorentz equation) by observing the ratio $R \equiv |\dot{\vec{p}}| / |\vec{E}|$ during the course of the collision. What was noted is as follows.

We describe first the collisions at capture threshold for which $\gamma_F = 1$. The ratio R starts close to 1 at t_I, increases to a maximum, then drops through 1 just before the point of closest approach ($r = r_{\min}$ at, say, $t = t_{\min}$), reaches a minimum shortly afterwards, and then gradually increases to 1 again as $t \to \infty$. (It is notable that the maximum rate of radiation occurs at or very near to the point where R passes through 1 for *all* the cases computed; the sign of $\vec{a} \cdot \vec{v}$ always changes before $t_{\min}$.) For values of b_I as low as 0.2, the minimum in R that occurs just after $t_{\min}$ is $R \simeq 0.12$.

However, the behavior in R for $t < t_{\min}$ is much more dramatic. When b_I has decreased to $\lesssim 3$, two peaks for $R > 1$ develop. The first, closest to $t_{\min}$ eventually increases apparently without limit as b_I is decreased. The second peak in $R \lesssim 1.3$ occurs before $\vec{a} \cdot \vec{v}$ changes sign and apparently decreases as b_I is decreased. The intermediate minimum, which eventually dips even below 1, apparently occurs when $\vec{a} \cdot \vec{v}$ changes sign. This sign change occurs earlier and earlier as b_I is decreased. As b_I decreases from 50 to 0.2, the primary peak in R increases from about 1 to about 2×10^{11} and occurs before $t_{\min}$ with distances to $r_{\min}$ increasing from very small values to about 10^6 before collision, with $\vec{a} \cdot \vec{v}$ eventually changing sign at least an order of magnitude farther away. The secondary peak becomes lost in the accuracy of the calculation and in any event seems to play no important role in the calculations. Meanwhile, the peak rate of radiation emitted increases from $\leq 10^{-4}$ to $\geq 10^2$. This peculiar behavior, which appears ever less physical as b_I is made smaller, is consistent with our recently published results for $b_I = 0$,[10] for which there are no physical solutions with finite initial values. It seems to herald the breakdown of the Lorentz-Dirac equation as b_I becomes less than approximately one classical electron radius.

The behavior when the initial particle kinetic energy is 550 MeV is comparable, but less dramatic because there is a minimum in $b_I = 0.4255$ below which there is capture. The largest value of b_I was $\simeq 60$ units. Even for this value the minimum value of R just after $t_{\min}$ was $\simeq 0.10$. As above, the ratio passed through 1 at or near the time of peak rate of radiation. This minimum in R dipped to a value $\gtrsim 6 \times 10^{-3}$ for $b_I \simeq 2.5$ and then increased to $\simeq 0.23$ for the lowest value of $b_I = 0.4255$. The primary peak in R ranged from $\lesssim 4 \times 10^2$ for $b_I \simeq 60$ to $\simeq 2.5 \times 10^5$ for $b_I \lesssim 1.5$ and occurred at distances $r \gtrsim 1 \times 10^3$ before the collision. The secondary peak in $R \gtrsim 1.1$ was noticeable only for the larger values of b_I and occurred beyond where $\vec{a} \cdot \vec{v}$ changes sign, which was typically an order of magnitude beyond the primary peak in R. The peculiar behavior noted here seems to be indicating a breaking down of the Lorentz-Dirac equation even for values of b_I somewhat larger than unity.

VI. DISCUSSION AND CONCLUSIONS

The numerical solutions of the Lorentz-Dirac equation to treat the scattering of a spinless point particle in the static electric field of an oppositely charged massive point including radiation effects that we have presented here exhibit some very attractive yet perplexing features. We have given solutions for a fixed final particle energy ($\gamma_F = 1$) at capture threshold and for a fixed initial particle kinetic energy of 550 MeV ($\gamma_I = 1077.32$). In the first case, physical solutions exist apparently for all $b_I > 0$, but in the second case there is a minimum of $b_I = 0.4255$ below which capture ensues. A satisfying confirmation of numerical accuracy was that the loss in particle energy and the integrated Larmor energy radiated during the collision were

in excellent agreement for all the computations. Furthermore, in both instances, the solutions approach those of the Lorentz equation (no radiation reaction) in the limit of large impact parameters, and for the somewhat larger values of b_I, the solutions were physically very reasonable, as evidenced by the amount of energy lost to radiation, the behavior of the angular momentum, and its loss to radiation and the angle scattered through. Typical trajectories for particles having the same initial conditions with radiation included make physical sense when compared with those without radiation.

However, difficulties arise when the impact parameter is decreased to its limit. For the second case of a fixed initial-particle energy, we have noted the marked disagreement between the calculated differential scattering cross section with those of the relativistic Rutherford results. We have also seen the strange behavior in the increase in the ratio $|\dot{\vec{p}}|/|\vec{E}|$ before the collision preceded by the sign change in $\vec{a}\cdot\vec{v}$ at increasingly large distances from the scattering center. This unusual behavior is even more pronounced for the first case of fixed final energy, where apparently b_I can be decreased to zero. In this limit, the scattering angles decrease, but the incident energy and energy radiated, the initial angular momentum and its change, the peak ratio $|\dot{\vec{p}}|/|\vec{E}|$, the distance where it occurs, and the greater distance where $\vec{a}\cdot\vec{v}$ changes sign (with the undesirable implication that the particle accelerates *away* from the attractive center even at very large distances) *all* increase with apparently no limit. If the criterion for breakdown of the Lorentz-Dirac equation is b_I for which about one electron mass is radiated away, this occurs for $b_I \simeq 2.9$ in the first case and for a somewhat large value of $b_I \simeq 44$ in the second case. While the above-mentioned features are undesirable, they are consistent with our results found previously that no physical solutions exist in the attractive case for finite initial conditions in distance, energy, and acceleration when $b_I = 0$. The difficulty there occurs when a singularity actually lies on the true trajectory. According to these extended results for the Lorentz-Dirac equation, the particle "knows" well ahead of time of a singularity directly on, or even nearly on the track. Certainly, according to quantum mechanics, it is impossible to prepare a path with an impact parameter precisely zero. However, classically, it would be considerably more satisfying if these difficulties did not arise. One suspects that these undesirable aspects can be eliminated by effectively removing the singular field at the point source, for example, by considering only effectively extended charges.[16,17]

ACKNOWLEDGMENTS

This research was supported by the National Research Council of Canada. One of us (W.E.B.) wishes to thank the Max Planck Institut für Strömungsforschung, 34 Göttingen, West Germany for hospitality while a portion of this work was done.

APPENDIX: RELATIVISTIC RUTHERFORD SCATTERING AND DIFFERENTIAL SCATTERING CROSS-SECTION FORMULA

The relativistic differential equation for the orbit of a spinless particle of charge $(-e$ say) in the fixed Coulomb static field due to a massive particle of opposite charge $(+e)$ is[15] (with $e = c = m = 1$)

$$\frac{d^2s}{d\varphi^2} + \lambda^2 s = D\,, \tag{A1}$$

where $s \equiv 1/r$, $D = W/L^2$, $W = \gamma - 1/r = \gamma_I = \gamma_F$ is the total particle energy (a constant of the motion), $L = \gamma r^2\dot{\varphi} = \gamma_I v_I b_I$ is the orbital angular momentum of the particle (also a constant of the motion), and $\lambda^2 = 1 - 1/L^2$, $(L > 1)$. The solution of Eq. (A1), when the line from which the polar angle φ is measured is such that $\varphi = 0$ at a perihelion, is

$$s \equiv \frac{1}{r} = A\cos(\lambda\varphi) + \frac{D}{\lambda^2}\,, \tag{A2}$$

where $A = (W^2 - \lambda^2)^{1/2}/L\lambda^2$. When $L < 1$, the solution is

$$s \equiv \frac{1}{r} = A\cosh(\lambda\varphi) - \frac{D}{\lambda^2}\,, \tag{A3}$$

where now $\lambda^2 = 1/L^2 - 1$ and $A = (W^2 + \lambda^2)^{1/2}/L\lambda^2$. Equation (A2) or (A3) gives the additional scattering at the ends of the computation as mentioned in Sec. II. The asymptotic directions are given by

$$\cos(\lambda\alpha) = -\frac{D}{A\lambda^2} \quad \text{or} \quad \alpha = \pm\frac{1}{\lambda}\cos^{-1}\left(\frac{-D}{A\lambda^2}\right). \tag{A4}$$

To derive the relativistic Rutherford scattering formula, we can greatly simplify matters when $L \gg 1$ so that $\lambda \approx 1$. (Recall that for the case of initial kinetic energies of 550 MeV, the initial angular momentum ranged from a minimum of 458.4 to $\gtrsim 6.5 \times 10^4$.) The scattering angle, θ, is given by $\theta = 2\alpha - \pi$ or $\theta/2 = \alpha - \pi/2$, where, to a very good approximation,

$$\alpha = \frac{1}{\lambda}\cos^{-1}\frac{-D}{A\lambda^2} \simeq \cos^{-1}\frac{-W}{L(W^2-1)^{1/2}}\,. \tag{A5}$$

Then $\tan(\theta/2) = -\cot\alpha = W/[L^2(W^2-1) - W^2]^{1/2}$, and $L = (W^2-1)^{1/2}b_I$. Defining $d\sigma = 2\pi b_I db_I$ with $d\Omega = 2\pi \sin\theta d\theta$, and proceeding as in the usual nonrelativistic case, results in the relativistic Rutherford scattering formula,

$$\frac{d\sigma}{d\Omega} \simeq (-)\frac{W^2}{4(W^2-1)^2}\frac{1}{\sin^4(\frac{1}{2}\theta)} \tag{A6}$$

in units of $(e^2m^{-1}c^{-2})^2$ per sr, and W is the total energy in electron rest mass units. If $W \gg 1$, as is the case here, then

$$\frac{d\sigma}{d\Omega} \simeq \frac{1}{4W^2}\frac{1}{\sin^4(\frac{1}{2}\theta)} . \tag{A7}$$

[1]Tse Chin Mo and C. H. Papas, Phys. Rev. D 4, 3566 (1971).
[2]W. B. Bonnor, Proc. R. Soc. London A337, 591 (1974).
[3]J. C. Herrera, Phys. Rev. D 15, 453 (1977).
[4]M. Sorg, Z. Naturforsch. 29A, 1671 (1974).
[5]M. Sorg, Z. Naturforsch. 31A, 1133 (1976).
[6]J. Huschilt, W. E. Baylis, D. Leiter, and G. Szamosi, Phys. Rev. D 7, 2844 (1973).
[7]J. Huschilt and W. E. Baylis, Phys. Rev. D 9, 2479 (1974).
[8]W. E. Baylis and J. Huschilt (unpublished).
[9]J. Huschilt and W. E. Baylis, Phys. Rev. D 13, 3256 (1976).
[10]W. E. Baylis and J. Huschilt, Phys. Rev. D 13, 3262 (1976).
[11]P. A. M. Dirac, Proc. R. Soc. London A167, 148 (1938).
[12]F. Rohrlich, *Classical Charged Particles* (Addison-Wesley, Reading, Mass., 1965).
[13]F. Rohrlich, in *Physical Reality and Mathematical Description*, edited by C. P. Enz and J. Mehra (Reidel, Boston, Mass., 1974), p. 387.
[14]J. D. Jackson, *Classical Electrodynamics*, second edition (Wiley, New York, 1975), p. 660.
[15]R. D. Sard, *Relativistic Mechanics* (Benjamin, New York, 1970), p. 189.
[16]See for example J. Petzold and M. Sorg, Z. Phys. A283, 207 (1977).
[17]See also W. Heudorfer and M. Sorg, Z. Naturforsch. 32A, 685 (1977), and references therein.